Effects of linking up of discontinuities on fracture growth and groundwater transport

Agust Gudmundsson · Otilie Gjesdal
Sonja L. Brenner · Ingrid Fjeldskaar

Abstract It is proposed that the growth of fractures is the basic process for generating and maintaining permeability in solid rock (bedrock). Many extension fractures grow as hydrofractures, whereas many shear (and extension) fractures grow through the formation of transverse fractures that connect the adjacent tips of existing fractures. In a boundary-element analysis, the hydrofractures are modeled as being driven open by a fluid overpressure that varies linearly from 10 MPa at the fracture centre to 0 MPa at the fracture tip. The host rock has a uniform Young's modulus of 10 GPa, a Poisson's ratio of 0.25, and is dissected by vertical joints and horizontal contacts, each of which is modeled as an internal spring of stiffness 6 MPa m^{-1}. The number of joints and contacts, and their location with respect to the hydrofracture tip are varied in different model runs. The results of the analyses indicate that the tensile stresses generated by overpressured hydrofractures open up joints and contacts out to considerable distances from the fracture tip, so that they tend to link up to form a hydraulic pathway. Using the same Young's modulus, Poisson's ratio, and internal spring constant for joints as in the hydrofracture models, boundary-element models were made to study the interaction stresses that cause neighbouring joints to become interconnected through the growth of linking transverse fractures that, ultimately, may evolve into shear fractures. The models were subjected to tensile stress of 6 MPa acting normal to the joint planes as the only loading. The offset (horizontal distance) and underlap (vertical distance) between the adjacent tips of the joints were varied between model runs. The results show a concentration of tensile and shear stresses in the regions between the neighbouring tips of the joints, but these regions become smaller when the underlap of the joints decreases and changes to overlap. These stress-concentration regions favour the development of transverse (mostly shear) fractures that link up the nearby tips of the joints, so as to form a segmented shear or extension fracture. Analytical results on aperture variation of a hydrofracture in a homogeneous, isotropic rock are compared with boundary-element results for a hydrofracture dissecting layered rocks. The aperture is larger where the hydrofracture dissects soft (low Young's modulus) layers than where it dissects stiff layers. Aperture variation may encourage subsequent groundwater-flow channeling along a pathway generated by a hydrofracture in layered rocks.

Received: 10 August 2001 / Accepted: 11 November 2002
Published online: 15 January 2003

A. Gudmundsson (✉) · O. Gjesdal · S. L. Brenner · I. Fjeldskaar
Geological Institute, University of Bergen,
Allegt. 41, 5007 Bergen, Norway
e-mail:
agust.gudmundsson@geol.uib.no, Agust.Gudmundsson@gwdg.de
Tel.: +47–55583521, Fax: +47-55589416

A. Gudmundsson
Department of Structural Geology and Geodynamics,
Geoscience Centre of the University of Göttingen,
Goldschmidtstraße 3, 37077 Göttingen, Germany

Résumé Nous proposons que le développement des fractures est le processus de base qui génère et maintient la perméabilité des roches indurées de socle. De nombreuses fractures en extension se forment en tant qu'hydrofractures, tandis que de nombreuses fractures de cisaillement (et en extension) se développent par la formation de fractures transverses qui mettent en connexion les parois adjacentes de fractures existantes. Dans une analyse des éléments aux limites, les hydrofractures sont modélisées comme si elles étaient maintenues ouvertes par une surpression de fluide qui varie linéairement de 10 MPa dans la fracture à 0 MPa sur sa paroi. La roche magasin possède un module de Young uniforme de 10 GPa, un rapport de Poisson de 0.25, et est recoupée par des fractures verticales et des joints horizontaux, chacun étant modélisé comme une source interne avec une rigidité de 6 MPa m^{-1}. Le nombre de fractures et de joints et leur localisation par rapport aux parois de l'hydrofracture varient dans les différents traitements de modélisation. Les résultats des analyses indiquent que les contraintes de tension générées par les hydrofractures en surpression ouvrent les fractures et les joints sur des distances considérables à partir des parois de la fracture, de telle sorte qu'elles tendent à se connecter pour former un cheminement hydraulique. En utilisant le même module de Young, le même rapport de Poisson et la même constante de source interne pour les fractures que dans les modèles d'hydrofracture, des modèles d'éléments aux limites ont été élaborés pour étudier les contraintes

 DOI 10.1007/s10040-002-0238-0

d'interaction qui provoquent l'interconnexion de fractures voisines grâce à l'extension de fractures transverses qui, finalement, peuvent évoluer en fractures de cisaillement. Les modèles ont été soumis à un effort de traction de 6 MPa appliqué normalement aux plans de fracture comme unique charge. Le déplacement (en distance horizontale) et l'écartement (en distance verticale) entre les parois des fractures ont varié selon les différents traitements. Les résultats montrent une concentration de contraintes de tension et de cisaillement dans les secteurs entre les parois des fractures, mais ces secteurs se réduisent lorsque l'écartement des fractures diminue et devient un recouvrement. Ces zones de concentration des contraintes favorisent le développement de fractures transverses (principalement de cisaillement) qui mettent en relation les parois voisines des fractures de manière à former une fracture segmentée de cisaillement ou d'extension. Les résultats analytiques sur la variation de l'ouverture d'une hydrofracture dans une roche homogène et isotrope sont comparés aux résultats des éléments aux limites pour une hydrofracture recoupant des roches litées. L'ouverture est plus large lorsque l'hydrofracture recoupe des couches tendres (module de Young faible) que lorsqu'elle recoupe des couches rigides. La variation de l'ouverture peut favoriser la chenalisation pour un écoulement souterrain subséquent le long d'un cheminement généré par une hydrofracture dans des roches litées.

Resumen Se propone que el crecimiento de fracturas es el proceso básico de generación y mantenimiento de la permeabilidad en rocas sólidas (roca madre). Muchas fracturas extensivas crecen por fracturación hidráulica, mientras que muchas fracturas de cizalla (y extensivas) lo hacen mediante la formación de fracturas transversales que conectan los extremos adyacentes de fracturas existentes. Por medio de un análisis de elementos de contorno, se ha modelado el crecimiento de las fracturas hidráulicas por un exceso de presión, la cual varía linealmente entre 10 Mpa en el centro de la fractura y 0 Mpa en el extremo. La roca madre tiene un módulo de Young uniforme de 10 Gpa, un coeficiente de Poisson de 0.25, y está diseccionada por diaclasas verticales y contactos horizontales que son modelados, cada uno de ellos, como fuente interna de rigidez igual a 6 MPa m^{-1}. El número de diaclasas y de contactos, así como su situación respecto al extremo de las fracturas hidráulicas, han sido modificados en diferentes pasadas del modelo. Los resultados de los análisis indican que las tensiones generadas por fracturas hidráulicas sobrepresionadas abren las diaclasas y contactos a distancias considerables del extremo de la fractura, de manera que tienden a unirse y a formar caminos o vías de flujo. Utilizando para las diaclasas el mismo módulo de Young, coeficiente de Poisson y manantial interno constante que se empleó en los modelos de fracturas hidráulicas, se ha elaborado modelos de elementos de contorno para estudiar las tensiones de interacción que causan la interconexión de diaclasas vecinas por medio del crecimiento de fracturas transversales de enlace, y que pueden llegar a convertirse en fracturas de cizalla. Los modelos fueron sometidos a tensiones de 6 Mpa normales a los planos de diaclasas como única carga. Se ha modificado el acomodo o distancia horizontal ("offset") y la distancia vertical ("underlap") entre extremos adyacentes de las diaclasas en las diversas pasadas del modelo. Los resultados muestran una concentración de tensiones y cizallas en las regiones situadas entre extremos vecinos de las diaclasas, pero estas regiones son menores conforme la distancia vertical de las diaclasas decrece y cambia a solapamiento de techo ("overlap"). Estas regiones de concentración de esfuerzos favorecen el desarrollo de fracturas transversales (mayoritariamente de cizalla) que enlazan los extremos vecinos de las diaclasas para formar una fractura segmentada de cizalla o extensiva. Se compara los resultados analíticos de la variación de la apertura de una fractura hidráulica en una roca homogénea e isótropa con los resultados del modelo de elementos de contorno en fracturas hidráulicas que diseccionan rocas estratificadas. La apertura es mayor si la fractura hidráulica disecciona capas deleznables (módulo de Young pequeño) que cuando lo hace en capas rígidas. La variación de la apertura puede favorecer el acanalamiento del flujo de aguas subterráneas a lo largo de caminos generados por una fractura hidráulica en rocas estratificadas.

Keywords Hydrofractures · Rock discontinuities · Fracture growth · Fluid transport · Hydrogeology

Introduction

Flow of fluids in solid rocks is commonly very different from flow in sediments. Most solid rocks contain systems of fractures due to tectonic forces, occasionally the result of excavations, which bound blocks of intact rock. In crystalline rocks, the intact rock has normally such a low permeability that groundwater flow occurs mainly along joints, faults, contacts, and other discontinuities. This means that the flow of water in the rock is largely determined by the distribution of interconnected fractures and the way in which their apertures respond to the associated stress field.

All tectonic fractures are either primarily extension fractures or shear fractures. These can be distinguished based on the relative displacement across the fracture plane. In an extension fracture the displacement is perpendicular to, and away from the fracture plane; in a shear fracture the displacement is parallel with the fracture plane. Extension fractures grow in a direction perpendicular to the minimum principal compressive stress (considered positive). They include two main types: tension fractures and hydrofractures. Tension fractures form when the minimum principal compressive stress is negative. They are mostly limited to shallow depths in areas undergoing active extension, such as rift zones (Gudmundsson 1992). By contrast, hydrofractures can form at any depth, provided the total fluid pressure is

 DOI 10.1007/s10040-002-0238-0

equal to the sum of the minimum principal stress and the tensile strength of the rock. They comprise fractures driven open by any kind of fluid, such as magma (dykes, sheets, and sills), geothermal water (mineral veins), oil, gas, and groundwater (some joints).

Shear fractures with significant displacements are referred to as faults. They are commonly major water conduits (Bruhn et al. 1994; Caine et al. 1996; Evans et al. 1997; Haneberg et al. 1999; Faybishenko et al. 2000). Many faults develop from smaller fractures, commonly sets of joints and extension fractures (Gudmundsson 1992; Cartwright et al. 1995; Crider and Pollard 1998; Acocella et al. 2000). The permeabilities of fracture sets and faults change much during their development. The state of stress in a particular area controls the activity of existing faults and fracture sets and may also initiate new, water-conducting fractures. Many old fracture sets and faults are reactivated when the controlling stress field changes, in which case they may increase the temporary average permeability of a site by several orders of a magnitude (Gudmundsson 2000a). The overburden pressure may also affect the apertures of fractures. Although considerable progress has been made in recent years concerning the general effect of normal and shear stresses on the permeability of a rock mass, these effects appear complex (Gentier et al. 2000) and the details are still not well understood.

This paper has three principal aims. First, to summarise general field data on extension fractures and shear fractures (faults) as a basis for modeling. These data are taken from several areas studied by the authors, but primarily from Iceland, England, and Norway. The second aim is to develop analytical and numerical models of extension fractures and shear fractures. Here the focus is on their growth. In particular, new numerical models are presented of the growth of fractures through linking up of existing discontinuities such as contacts and joints in the host rock. Also provided are analytical and numerical models of aperture variations of extension fractures and how these may reflect the mechanical properties of a layered host rock. The third aim is to present some general analytical models of fluid flow in fractures, based on the field data and the results of the modeling.

Field Examples of Extension Fractures

Tension Fractures

One of the two main types of extension fractures is the tension fracture (Fig. 1). A tension fracture forms when there is an absolute tension in the crust; that is, when the minimum principal compressive stress is negative. Tension fractures occur normally only at, or close to, the earth's surface. They are particularly common in areas undergoing active extension, such as in rift zones and grabens at divergent plate boundaries. Under such conditions, it follows from the Griffith criterion (Paterson 1978) of fracture initiation that the maximum depth, d_{max}, to which a surface-tension fracture propagates before changing into a normal fault, a shear fracture, is (Gudmundsson 1992, 1999):

Fig 1 Tension fracture conducting groundwater in the Thingvellir Fissure Swarm of the Holocene rift zone in Southwest Iceland (cf. Gudmundsson 1987a, 2000b). View northeast; the host rock is a basaltic pahoehoe lava flow. Matching jogs and notches, and other considerations, indicate that this fracture is a pure tension fracture with surface aperture of as much as 10 m and groundwater depth of tens of metres

$$d_{\max} = \frac{3T_0}{\rho_r g} \quad (1)$$

where T_0 and ρ_r are the in-situ tensile strength and density respectively of the host rock, and g is the acceleration due to gravity. For a tension fracture such as the one in Fig. 1, the average host-rock density is around 2,300 kg m^{-3} and the in-situ tensile strength may vary in the range 0.5–6 MPa (Gudmundsson 1999). Using 9.8 m s^{-2} for g, Eq. (1) gives the maximum depth of a tension fracture before it would change into a normal fault, as around 70 m (for T_0=0.5 MPa) and 800 m (for $T_0 = 6$ MPa).

When a tension fracture (Fig. 1) changes into a normal fault, the fault may remain open at the surface (Fig. 2). This is because the uppermost part of the fault

 DOI 10.1007/s10040-002-0238-0

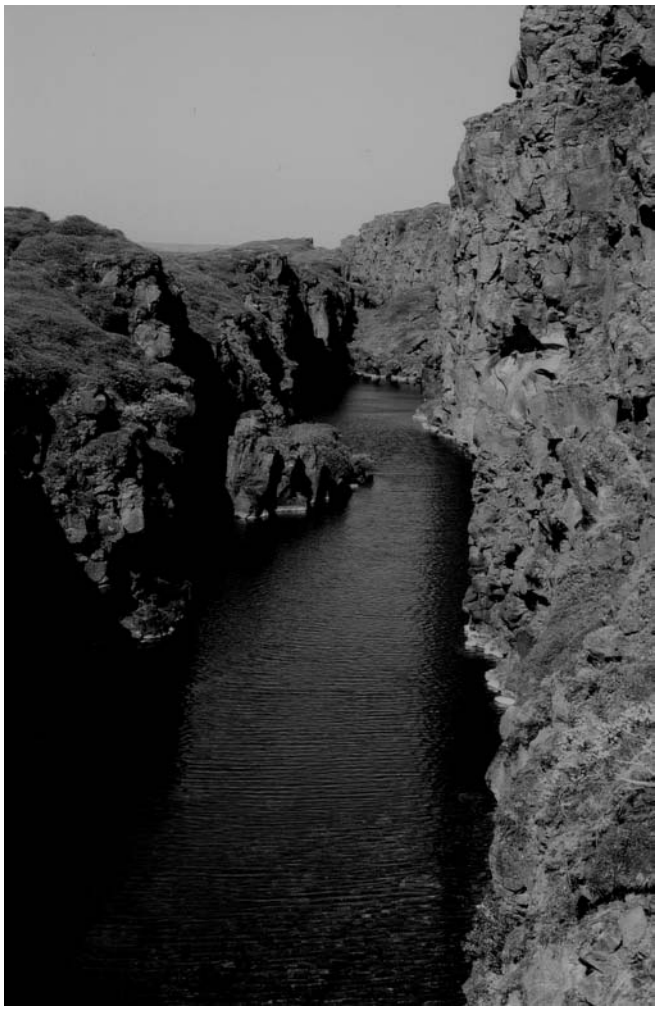

Fig. 2 Normal fault conducting groundwater in Krafla Fissure Swarm of the Holocene rift zone of North Iceland (cf. Gudmundsson et al. 2002, Fig. 8). The aperture of the fracture is similar to that in Fig. 1, but the left wall has subsided relative to the right wall. View north; the host rock is a basaltic pahoehoe lava flow

may still be subject to an absolute tension, at least during rifting episodes, which keeps the uppermost part of the fault open. Normal faults and tension fractures formed under these conditions have commonly very large apertures at and near the surface (Figs. 1, 2) and may transport large volumes of groundwater.

Hydrofractures

Most extension fractures that are not tension fractures are hydrofractures, that is, fractures that are partly or entirely generated by an internal fluid overpressure, P_0. Overpressure is the pressure available to drive the fracture open and is defined as:

$$P_0 = P_t - \sigma_n \quad (2)$$

where P_t is the total fluid pressure, and σ_n is the normal stress on the hydrofracture. Most hydrofractures appear to be extension fractures (Gudmundsson et al. 2002), in which case the normal stress is equal to the minimum

Fig. 3 Set of calcite veins on the Somerset coast of the Bristol Channel, England (cf. Peacock and Sanderson 1999). The veins form a regular system, seen here in an eroded, lateral surface of a limestone outcrop. Most veins cross-cut without fracture-parallel displacement, indicating that they are extension fractures. View vertical; the hand of the person provides a scale

principal compressive stress, that is, $\sigma_n = \sigma_3$. In the literature, the overpressure P_0 is variously referred to as driving pressure, driving stress, or net pressure (Gudmundsson et al. 2002). It should not be confused with abnormal pore-fluid pressure in rock formations. Then, the hydrostatic pressure is commonly regarded as normal, and formation pressures lower than hydrostatic are referred to as subnormal or subpressures whereas pressures higher than hydrostatic are referred to as supernormal or surpressures (Selley 1998; Chilingar et al. 2002).

In many hydrofractures, such as those generated by gas, oil, and groundwater pressure, the fluid may disappear when the fracture has formed. These fluids are presumably responsible for the formation of many joints, as initially suggested by Secor (1965) and discussed in standard textbooks (Twiss and Moores 1992; van der Pluijm and Marshak 1997). Other hydrofractures, however, are generated by fluids that freeze or otherwise solidify in the fracture subsequent to its formation. These hydrofractures include magma-driven fractures such as dykes, sills, and inclined sheets, as well as mineral veins. Of these, perhaps the most relevant, and easiest to study, are mineral veins.

Mineral veins represent fluid flow in palaeohydrothermal systems (Gudmundsson et al. 2002). When the aspect ratio (length/aperture) of a vein is known, as well as the mechanical properties of its host rock, an estimate can be made of the fluid overpressure at the time of vein emplacement as well as the depth of origin of the fluid that formed the vein (Gudmundsson et al. 2002). Although some veins are members of dense, interconnected networks (Fig. 3), other veins appear isolated (Fig. 4). Many veins become arrested at contacts between layers of different mechanical properties (Fig. 4), whereas those that propagate through layered rocks are likely to show variation in aperture.

 DOI 10.1007/s10040-002-0238-0

Fig. 4 Calcite veins in a sea cliff at the Somerset coast of the Bristol Channel, England (cf. Peacock and Sanderson 1999). The veins are located in limestone. The vein tips became arrested when they propagated from the stiff limestone into the soft marl layers above and below the limestone. View east–southeast; the length of the steel tape is 0.5 m

Field Examples of Shear Fractures

Good examples of linking up of fractures into small-displacement shear fractures or faults occur in gneiss on the islands of Sotra and Øygarden off the coast of west Norway near the city of Bergen (Figs. 5, 6). The gneiss is well exposed and allows the fractures and faults to be observed in horizontal and vertical sections. In horizontal sections, many of the original extension fractures or joints from which the faults develop have an en-echelon arrangement (Fig. 5). Subsequently, the extension fractures link up by the growth of transverse fractures between the nearby tips of the original fractures. When all the original extension fractures have linked up, they form an interconnected system, thereby reaching the percolation threshold for fluid flow. Commonly, such segmented yet interconnected fracture systems behave mechanically as single fractures (Sneddon and Lowengrub 1969).

When subvertical extension fractures link up and increase their lateral lengths (strike dimensions), they normally also increase their depths (dip dimensions; Gudmundsson 2000b). When such a set of interconnected extension fractures reaches the depth given by Eq. (1), they change into normal faults, as is indicated by field examples (Figs. 1, 2, 7, and 8) and models for normal faults in the rift zone of Iceland (Gudmundsson 1992).

In vertical sections, the growth of small faults across mechanical layers is also indicated by examples from west Norway (Fig. 6). Normally, fractures have difficulty in crossing open, subhorizontal discontinuities, as are exemplified by exfoliation (sheets, sheeting) fractures in the gneiss in west Norway (Fig. 6). Exfoliation fractures form as a result of high compressive stresses. In west Norway, such stresses may have been generated during rapid erosion by glaciers, or alternatively as a result of deglaciation and associated postglacial uplift and bending (Gudmundsson 1999).

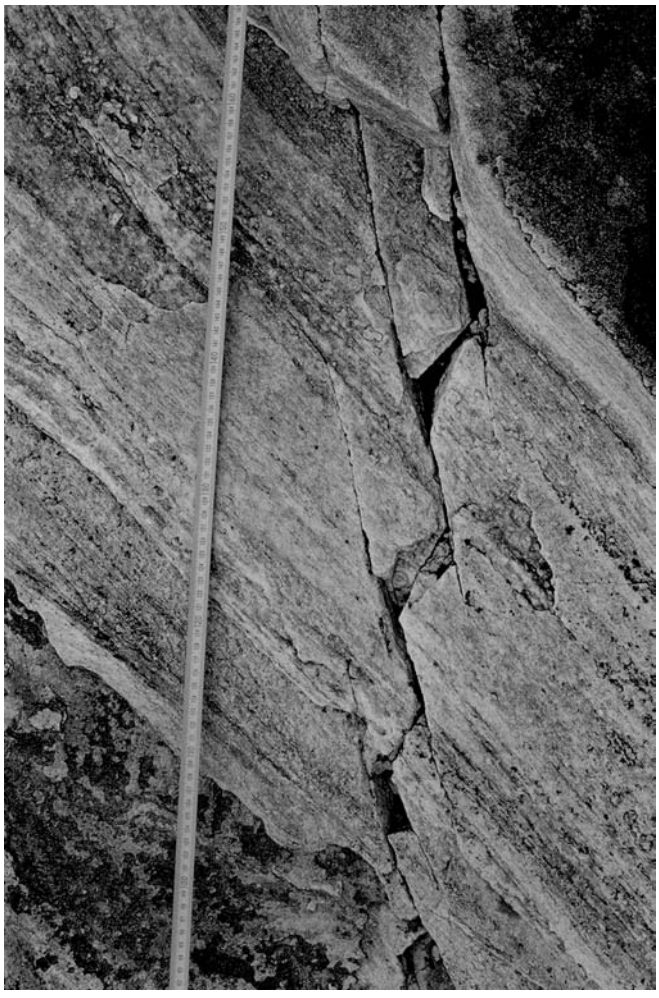

Fig. 5 Interconnected fracture set in gneiss on the island of Øygarden, West Norway. The length of individual fractures is up to 0.3 m, whereas that of the whole system is around 2.5 m (only the central part of which is seen here). The original en-echelon extension fractures are interpreted as having been short and underlapping, but subsequently became linked through transverse fractures into an interconnected set. The original en-echelon arrangement may have been due to an underlying weakness, an old discontinuity, making less than a right angle to the direction of σ_3 during the extension-fracture formation. For example, old weaknesses, such as normal faults buried under young lava flows, that trend oblique to the current direction of σ_3, are known to give rise to surface extension fractures with an en-echelon arrangement in the rift zone of Iceland (Gudmundsson 1987a). During further evolution of the set, some of the original extension fractures propagated their tips beyond the junctions with the transverse fractures. The same kind of development is common, at a much larger scale, at ridge segment–transform fault junctions (Gudmundsson et al. 1993). View north–northwest, parallel with the trend of the set; the length of the steel tape is around 0.8 m

The process of linking up of segments and growth of shear fractures at various scales, including large faults, is reviewed by Pollard and Segall (1987), Crider and Pollard (1998), Acocella et al. (2000) and Mansfield and Cartwright (2001). The general process is that fractures link up at different scales into larger and larger segments of the main fault. For strike-slip faults, the linking

 DOI 10.1007/s10040-002-0238-0

Fig. 6 Development of shear fractures in a vertical section through a mechanically layered host rock, gneiss, on the island of Øygarden, West Norway. Some of the mechanical layers, mainly generated by exfoliation, coincide with the primary layers of alternating dark amphibolite and light quartzo-feldspatic gneiss. The main shear fracture (just to the right of the centre of the photograph) strikes N45°E, and it has an average dip of 72°NW and a vertical displacement of 4 cm. The shear fracture tends to be somewhat steeper in the stiffer (high Young's modulus) layers. View northeast; the length of the steel tape is 0.2 m

Fig. 7 Oblique aerial photograph of a part of the Holocene Thingvellir Fissure Swarm in Southwest Iceland, showing normal faults that grow partly by linking up of gradually larger segments; linking up of kilometre-scale segments is seen where the main road crosses the fault to the right of the crossroad. These faults link up through hook-shaped tensile or hybrid fractures, rather than transverse-shear fractures, as is common in rift zones (Gudmundsson et al. 1993; Acocella et al. 2000). View southwest; the total length of the fault, which forms the western boundary fault of a 7-km-wide graben, is around 9 km. The surface aperture of the fault is up to 60 m, and its vertical displacement is as much as 40 m (cf. Gudmundsson 1987a, 2000b). To the west and east of the boundary fault, there are tension fractures, one of which (near the lake on the east side of the main fault) is seen in Fig. 1

up of fractures into larger segments is commonly a complex process (Cox and Scholz 1988; Bergerat and Angelier 2001). By contrast, for most dip-slip faults, particularly normal faults, the process of linking up is relatively simple (Figs. 7, 8).

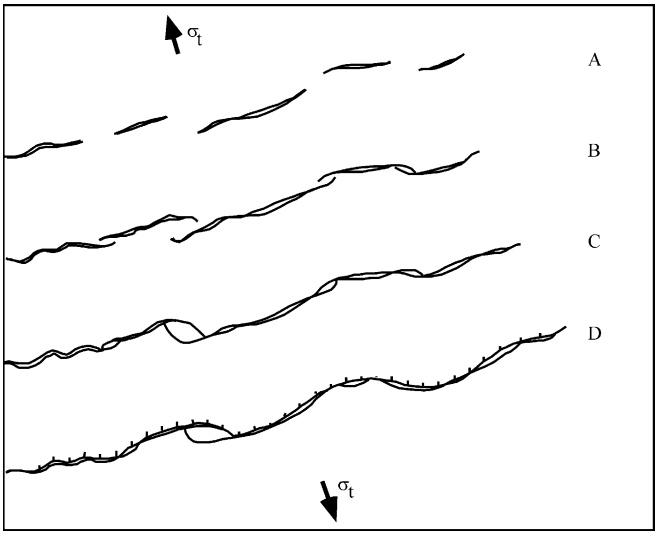

Fig. 8 Schematic illustration of the growth of tension fractures into a normal fault by lateral propagation and linking up of segments into larger structures (modified from Gudmundsson 1987b). As in Fig. 7, the linking up of fractures is here through hook-shaped, rather than transverse-shear, fractures. The model is based on actual observations in the Holocene rift zone of Iceland. The fractures are subject to a plate-pull-generated tensile stress, σ_t; stage *A* (a set of tension fractures) is the earliest result, and stage *D* (a normal fault) the most recent in the development

Modeling the Growth of Extension Fractures

Here the formation of a groundwater pathway through the linking up of discontinuities in the host rock is considered. The mechanism of pathway formation considered here is the propagation of a hydrofracture under internal fluid overpressure. This is the only loading applied. Numerical models were made of the pathway formation using the boundary-element program BEASY (1991). Well-known theoretical considerations suggest that hydrofractures are normally extension fractures (Anderson 1951; Hubbert and Willis 1957). For natural hydrofractures such as those resulting from the intrusion of dykes and mineral veins, this suggestion is generally supported by field observations (Pollard and Segall 1987; Gudmundsson 1995; Gudmundsson et al. 2002). Consequently, hydrofractures are here modeled as mode I cracks, that is, as pure extension (opening) fractures (Twiss and Moores 1992).

In each model, the internal fluid overpressure of the hydrofracture varies linearly from 10 MPa in the fracture centre (bottom of the model) to 0 MPa at the tip of the fracture (Fig. 9). This is believed to be an overpressure distribution suitable for many hydrofractures, particularly in layered host rocks, but the results are similar in the case of the overpressure being uniform (Gudmundsson et al. 2002). Only the upper half of each hydrofracture is modeled. Rigid-body translation and rotation are avoided by fastening the lower corners of each model by using the conditions of no displacement in the directions of the coordinate axes.

A typical Poisson's ratio of 0.25 is used in all the models (Johnson 1970; Jumikis 1979). A uniform

 DOI 10.1007/s10040-002-0238-0

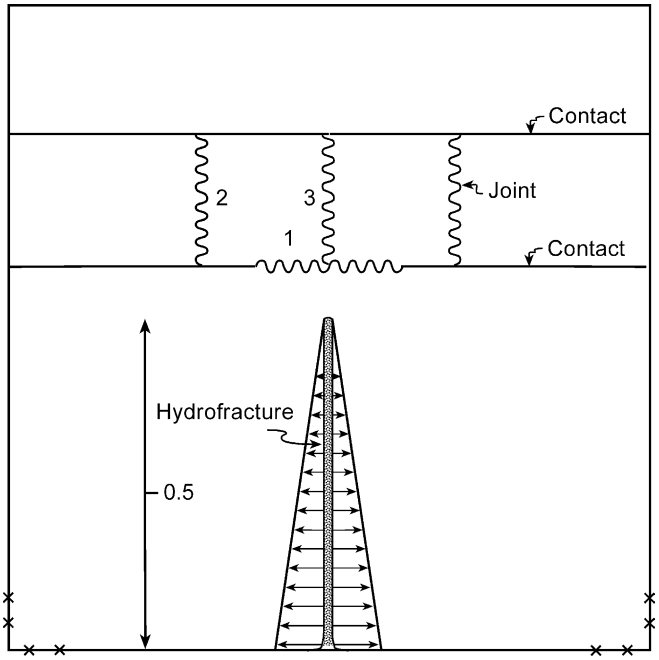

Fig. 9 General configuration of the boundary-element models in Figs. 10, 12, and 14. Horizontal contacts and vertical joints in the host rock are represented schematically by the pressure of internal springs (as indicated by the numbers *1–3*), and the linear-fluid overpressure distribution to which the hydrofracture is subjected is indicated by *horizontal arrows* of vertically decreasing lengths. These models are of unit height (the height of the hydrofracture being 0.5 unit) and fastened (subject to zero displacement), as indicated by the *crosses* in the lower corners. The host rock has a uniform Poisson's ratio of 0.25 and a Young's modulus of 10 GPa

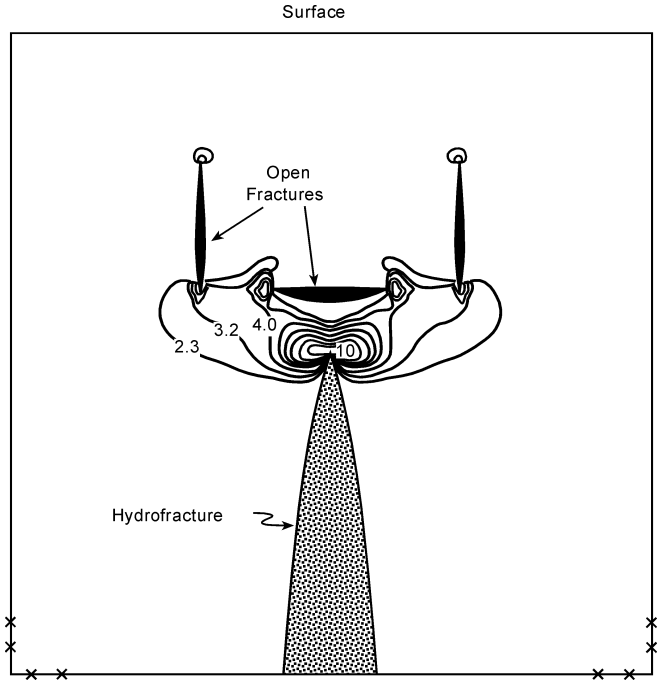

Fig. 10 Maximum tensile stress σ_3 in megapascals around the tip of a hydrofracture that opens up contacts and joints ahead of the tip (cf. Gudmundsson et al. 2002). In this and in subsequent models (Figs. 11, 12 and 14), only tensile stresses of 1–10 MPa are shown. In all the numerical models in this paper, tensile stresses are given as absolute values (magnitudes)

Young's modulus of 10 GPa is used, a value that corresponds to the lower range of laboratory values of Young's modulus for gneiss, 3–70 GPa (Johnson 1970; Jumikis 1979; Bell 2000). This low value is used because the in-situ values of Young's modulus are commonly much lower, particularly for near-surface rocks, than values for intact, small rock samples measured in the laboratory (Goodman 1989; Priest 1993).

The models differ largely in the location and size of the host-rock discontinuities, and the location of the tip of the hydrofracture with respect to the discontinuities. The term "discontinuity" is traditionally used for any type of mechanical break in a rock. In the models, however, most discontinuities represent either contacts or joints. Thus, for brevity, the vertical discontinuities are frequently referred to as joints, and the horizontal discontinuities as contacts. Each discontinuity is modeled as an internal spring with a stiffness ("strength") of 6 MPa m^{-1} (Fig. 9). Such a low value is assumed to be appropriate for a joint or extension fracture with a consolidated, elastic but soft infill, or a contact with weak sedimentary or pyroclastic material. These stiffness values are thought to be primarily appropriate for the upper part of a rift zone, such as in Iceland (Figs. 7, 8). For comparison, weak tuff layers, as are common in volcanic successions, have small-sample laboratory Young's moduli as low as 50 MPa, and weak mudrocks (e.g. marl) have Young's moduli as low as 3 MPa (Bell 2000). Numerical models have also been made with zero-discontinuity stiffness, corresponding to an open joint or contact, with results that are very similar to those for the stiffness of 6 MPa m^{-1} used here. In all the models, the lengths are given as fractions of the height which is a unit.

In the first model, the hydrofracture tip is at a depth of 0.5 unit below the free surface. This hydrofracture is approaching a horizontal contact and two vertical joints, all of which are represented by internal springs of length 0.2 unit (Fig. 10). The opening of the horizontal contact, which is greater than that of either vertical joint, is mainly due to downward deflection of its lower wall, whereas its upper wall remains essentially straight. This geometry is related to the Cook-Gordon mechanism for stopping cracks (Cook and Gordon 1964; Atkins and Mai 1985) and results, if the hydrofracture joins the contact, in a T-shaped fracture (Fig. 11). The high tensile-stress concentrations at all the tips of the opened-up contact and joints suggest that they tend to link up and grow further.

This linking up is seen in the next model (Fig. 12) where a vertical joint that is directly in line with the hydrofracture, but above the contact, has been added. The contact, here twice as long as the joints, has the greatest opening. All the three joints have similar openings which reach maximum values in the deeper parts of each joint. The central joint shows considerable opening although it is in a stress shadow of the much larger and more open contact. In this model, when the hydrofracture reaches

 DOI 10.1007/s10040-002-0238-0

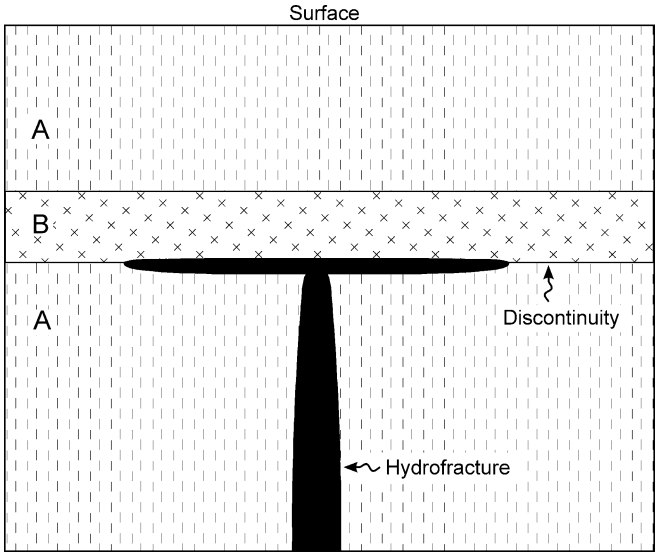

Fig. 11 Hydrofracture meeting with a weak contact may open it up and form a T-shaped fracture, particularly when the contact coincides with a strong contrast in stress, Young's modulus, or both, between the layers *A* and *B*

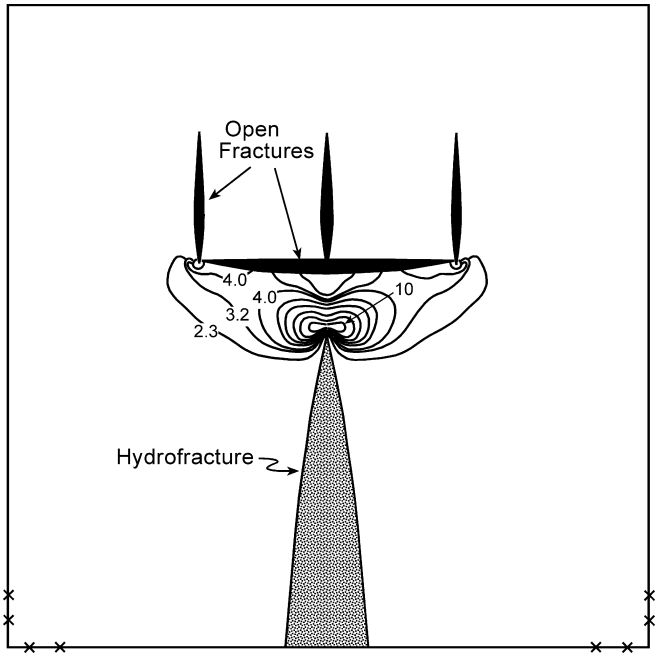

Fig. 12 Maximum tensile stress σ_3 around the tip of a hydrofracture that opens up contacts and joints ahead of the tip (cf. Gudmundsson et al. 2002). Location of the tip is as in Fig. 10 but here there are three weak joints (instead of two) and the weak contact is here twice as long as in Fig. 10

the contact it could continue its propagation along any of the joints. This type of hydrofracture growth is expected to be common in layered and jointed rock masses (Fig. 13), in which case more than one horizontal contact may open up simultaneously.

Such a development is seen in the next model (Fig. 14) which has three joints extending all the way to

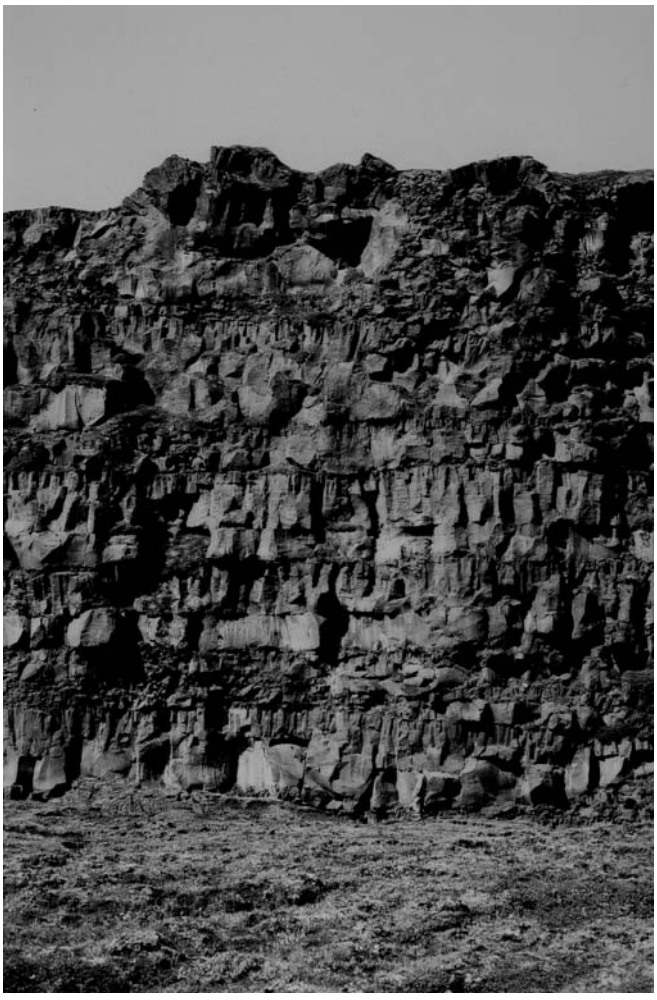

Fig. 13 Cross-section through the uppermost part of a thick pahoehoe lava flow in North Iceland showing horizontal contacts between flow units and vertical columnar (cooling) joints. Some contacts, or parts of contacts, are welded together, whereas most of the joints are open or with partial, weak infill. View west; the 20-m-high wall is a part of a normal fault that forms the western boundary of the Gjastykki Graben in the Krafla Fissure Swarm (cf. Gudmundsson 1995). The person at the foot of the wall, near the centre of the picture, provides a scale

the surface, a contact just above the hydrofracture tip, and another contact at a shallow depth. The model results show that the contact next to the tip has the greatest opening, but the upper contact also opens up. By contrast, the near-surface parts of the joints remain closed, whereas their deeper parts open up. These results are analogous to those obtained during the downward deflection of an elastic plate: its upper part becomes subject to horizontal compression whereas its lower part is subject to horizontal tension (Timoshenko and Goodier 1970).

Modeling the Linking up of Offset Joints

In this section examples are presented of the linking up of offset joints into interconnected fracture sets that may eventually develop into shear fractures and, then, major

 DOI 10.1007/s10040-002-0238-0

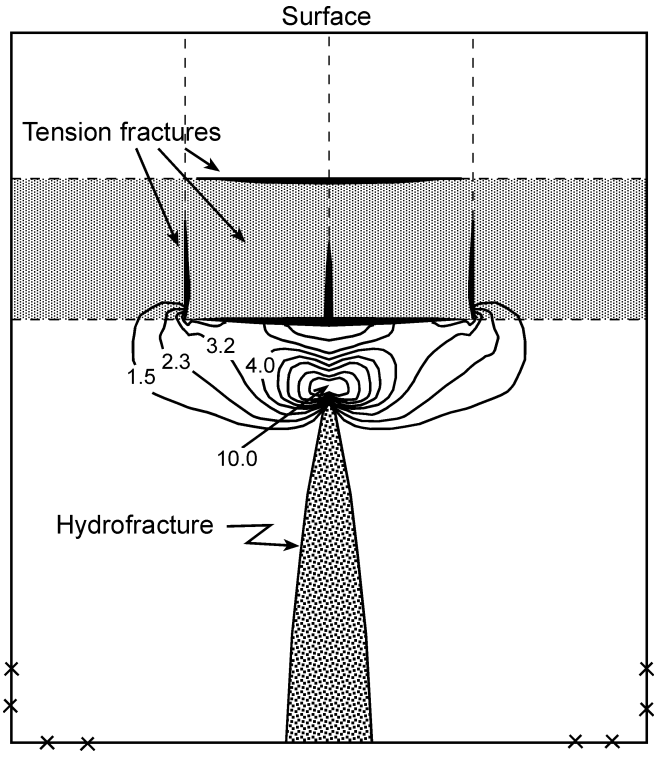

Fig. 14 Maximum tensile stress σ_3 around the tip of a hydrofracture that opens up contacts and joints as tension fractures ahead of the tip (cf. Gudmundsson et al. 2002). Location of the tip and joints is as in Fig. 12 but a new weak contact has been added at a shallow depth. This shallow contact opens up and contributes to vertical bending of the upper parts of the model, thereby closing the upper part of the joints

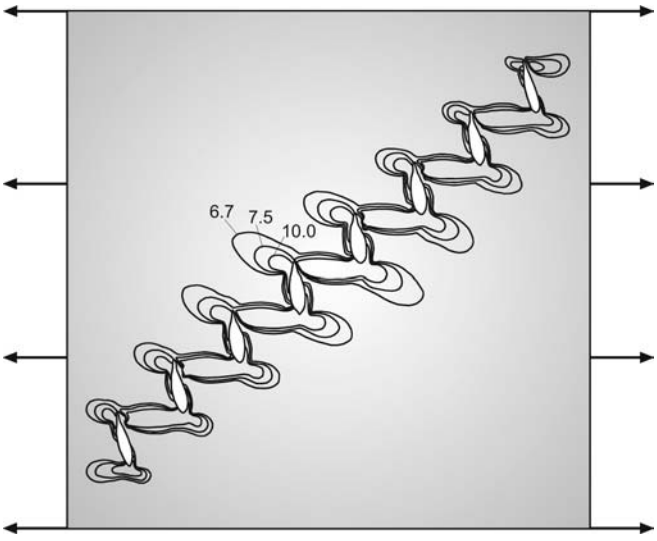

Fig. 15 Shear-stress concentration in megapascals generated around eight extension fractures subject to tensile stress of 6 MPa as the only loading. All the fractures are of equal length, 0.1 unit, and with equal spacing. Transverse-shear fractures would tend to develop in the high-stress concentration regions between the nearby tips of the extension fractures (cf. Fig. 5)

faults. All these models take as starting points field examples of evolving fracture systems and faults in West Norway, in particular on the islands of Sotra and Øygarden, west of the city of Bergen. All the models were run using the boundary-element program BEASY (1991).

In all the models, the only loading to which the fractures are subjected is horizontal tension of 6 MPa (Fig. 15). This value is used because the maximum in-situ tensile strength of gneiss is around 6 MPa (Amadei and Stephansson 1997). As is explained above, a uniform Young's modulus of 10 GPa for the gneiss is used, and a uniform Poisson's ratio of 0.25 (Johnson 1970; Jumikis 1979; Bell 2000). As in the earlier models (Figs. 10, 11, 12, and 14), all the extension fractures in these models are modeled as internal springs, each with a stiffness of 6 $MPam^{-1}$, corresponding to a joint with a soft infill or a contact with weak rocks.

With reference to Fig. 5, a general model of an en-echelon system subject to a tensile stress of 6 MPa is first presented. The model consists of eight extension fractures, each modeled as an internal spring. The model height is one unit. Each fracture has a length of 0.1 unit, and the upper and lower tips of each adjoining pair of fractures are at the same horizontal level. The underlap or vertical distance between the adjacent tips is thus zero, whereas the offset or horizontal distance between the adjacent tips is the same for all the fractures and equal to 0.1 unit.

The results (Fig. 15) show that there are stress-concentration regions between the adjacent tips of each pair of fractures. In these regions, there is concentration of shear stress and also tensile stress (not shown). This indicates that transverse fractures, many of which are shear fractures whereas others could be hybrid fractures, tend to develop between the adjacent ends of the extension fractures and link them up into a single, segmented fracture. When the initial en-echelon extension fractures become interconnected through transverse fractures, the percolation threshold of the fracture set is reached so that the fracture set acts as a single, segmented and interconnected cluster of fractures that can conduct groundwater from one end to the other. Such a development has already occurred in Fig. 5.

We also studied how sets of extension fractures link up when the underlap and offset between the adjacent tips of the original extension fractures vary (Fig. 16). This variation can be related to different arrangements of extension-fracture sources (points of initiation). These sources are often vesicles, pores, or other original weaknesses in the host rock that concentrate stresses and develop into extension fractures. In all these models, the vertical distance between the adjacent tips (the underlap) is denoted by c, the horizontal distance (the offset) by b, and the (constant) original length of individual fractures by a. All the fractures are subjected to a horizontal far-field tensile stress of 6 MPa.

The results (Figs. 17, 18, and 19) again show high-stress concentrations in the regions between the adjacent tips of the fractures. For the variation in underlap c, only the shear stress is presented (Fig. 17) but the tensile stresses are also high in roughly the same regions. The

 DOI 10.1007/s10040-002-0238-0

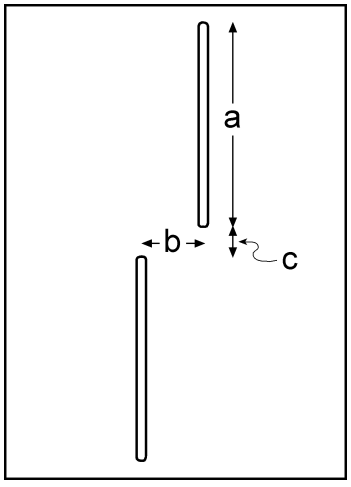

Fig. 16 General configuration of the boundary-element models in Figs. 17, 18 and 19. The extension fractures have equal lengths, *a*, offset *b*, and underlapping *c*. In all the models the length *a* is constant, but in some of the models the offset *b* varies, whereas in other models the underlapping *c* is the variable. In all the models, the fractures are subject to a tensile stress of 6 MPa as the only loading

models indicate that as long as the underlap between the adjacent tips of the fractures is greater than zero, the regions of high-stress concentration between the adjacent tips remain large and are likely to develop transverse fractures (Fig. 17). However, once the underlap starts to approach zero, and then becomes negative, so that the fractures become overlapping (not shown in Fig. 17), the stress-concentration regions shrink.

Photoelastic studies (Gudmundsson et al. 1993) support this conclusion; they show that once the underlap changes to an overlap, that is, when *c* becomes negative, the stress-concentration region between the nearby tips decreases in size. These results indicate that the most favourable configuration of offset extension fractures for the development of interconnecting shear fractures between the nearby ends is that of a significant underlapping. This conclusion is supported by the geometry of the en-echelon fracture set in Fig. 5. There the transverse fractures have developed while there was a significant underlapping of the original extension fractures.

As the offset *b* decreases, that is, when the original extension fractures become more nearly collinear, the shear-stress intensity decreases (Fig. 18), whereas the tensile-stress intensity increases (Fig. 19). Thus, collinear extension fractures have the greatest probability of in-plane propagation, which would lead to linking up (through extension fractures) of the nearby ends. Thus, the original configuration of the fractures in Fig. 5 favours shear-stress concentration and transverse-shear fractures, whereas collinear extension fractures favour tensile stresses and the growth of an extension fracture into a single, segmented fracture. In both cases, however, the tensile loading leads to stress concentrations that fa-

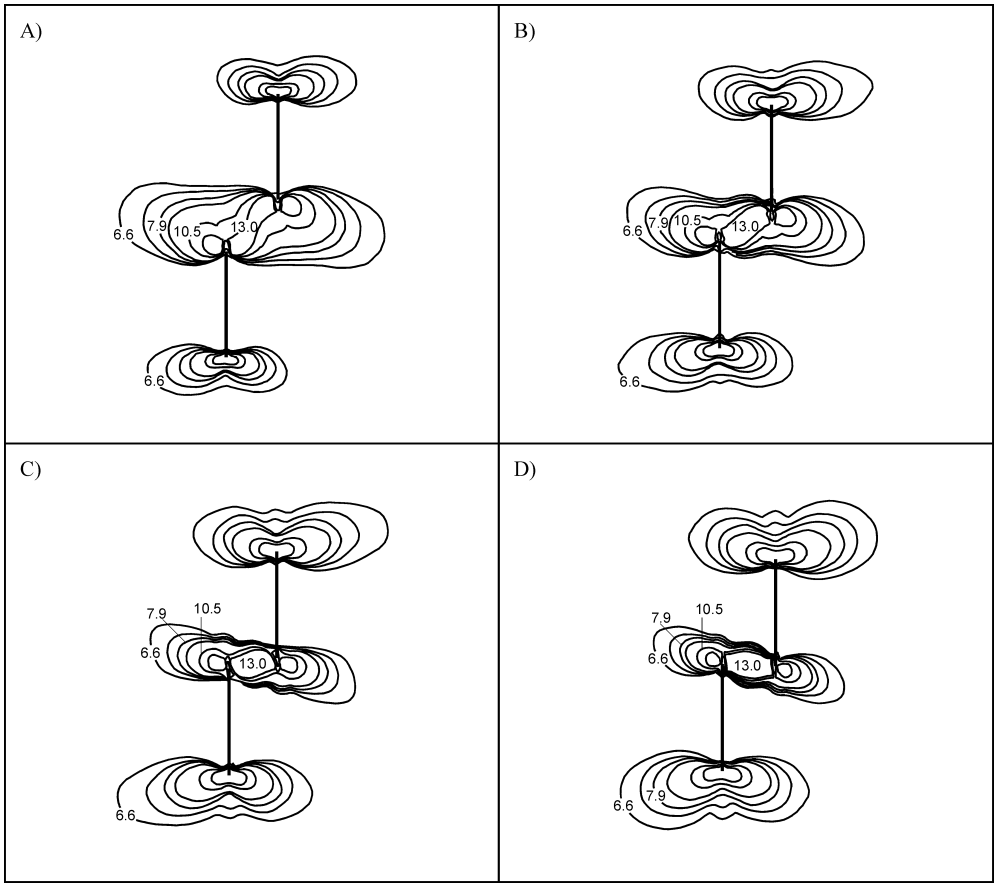

Fig. 17A–D Changes in shear-stress concentration between the extension fractures in Fig. 16 when the underlapping *c* changes, whereas the offset *b* is constant. In **A**, *c*=0.5*a* and *c* gradually decreases through **B** and **C** to 0*a* in **D**. The results show that the region of high shear-stress concentration gradually shrinks as the underlap decreases, whereas the shear stresses at the far tips increase

 DOI 10.1007/s10040-002-0238-0

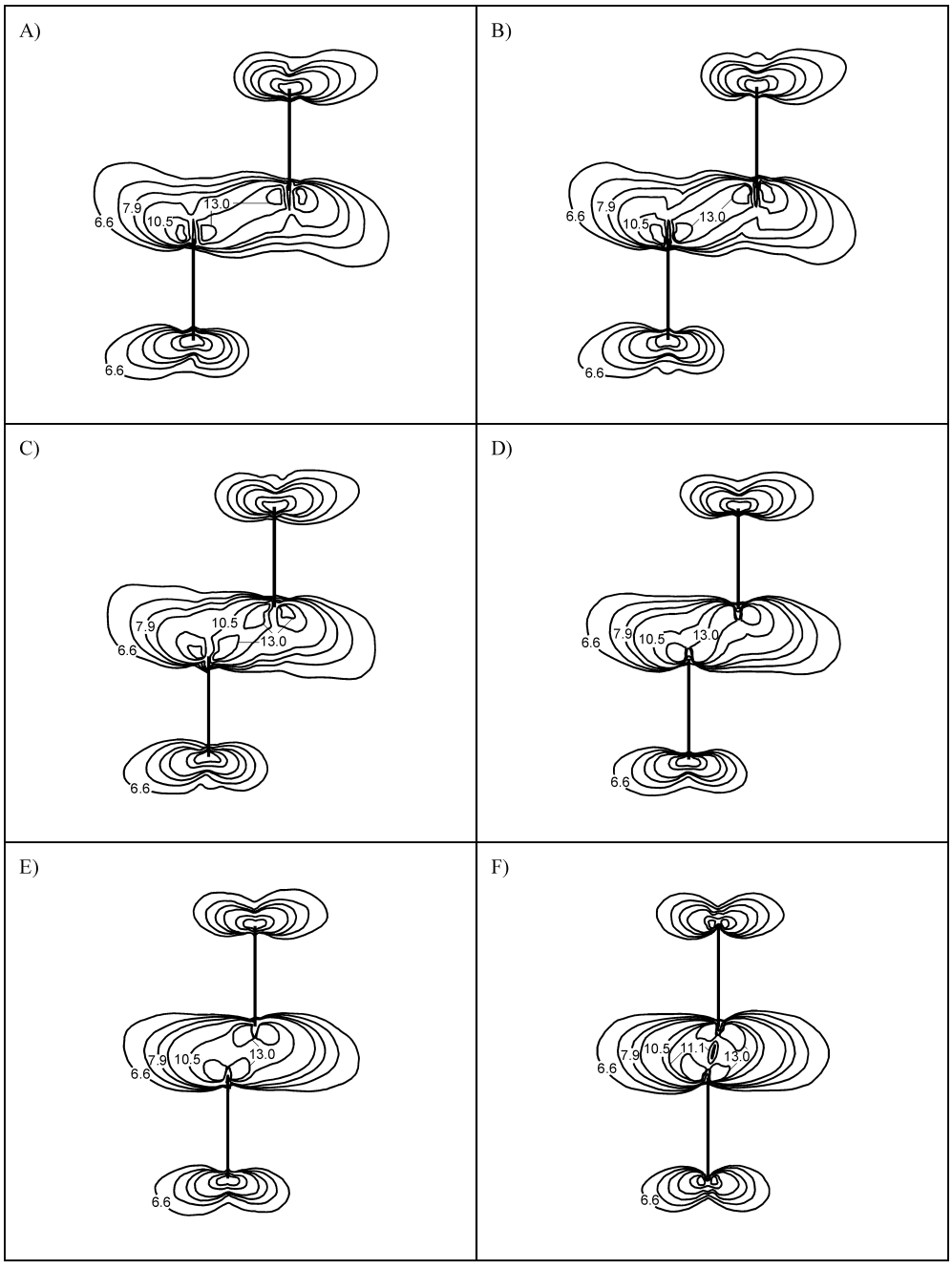

Fig. 18A–F Changes in shear-stress concentration between the extension fractures in Fig. 16 when the offset b changes whereas the underlap c is constant. In **A**, b=1.0a and b gradually decreases (through models **B**–**E**) to 0.1a in **F**. The region of high shear-stress concentration gradually shrinks as the offset decreases and the fractures become more nearly collinear

vour the linking up of the extension fractures – either into a fracture with en-echelon segments linked by transverse-shear fractures, or into a single, segmented (but collinear) extension fracture, depending on the configuration of the original extension-fracture set.

Groundwater Transport in Fractures

Volumetric Flow Rate

When either an original set of extension fractures has linked up through transverse fractures, or a cluster of fractures has become interconnected through linking up of contacts, joints, and other discontinuities in the host rock, the set or the cluster may act both mechanically and hydraulically as a single fracture. A crude estimate of the volumetric rate of flow of fluid through this fracture can be obtained, provided certain simplifications are made. The simplest case of fluid transport along extension fractures and shear fractures is considered, where the assumption is made that the source of the fluid is a horizontal aquifer (Fig. 20). However, the general conclusions from the modeling presented below do not depend on the assumption of a horizontal aquifer.

The case is considered where the aquifer is subject to internal fluid excess pressure p_e (in excess of the lithostatic pressure in the host rock at its upper contact with the aquifer). This excess pressure can be generated in

 DOI 10.1007/s10040-002-0238-0

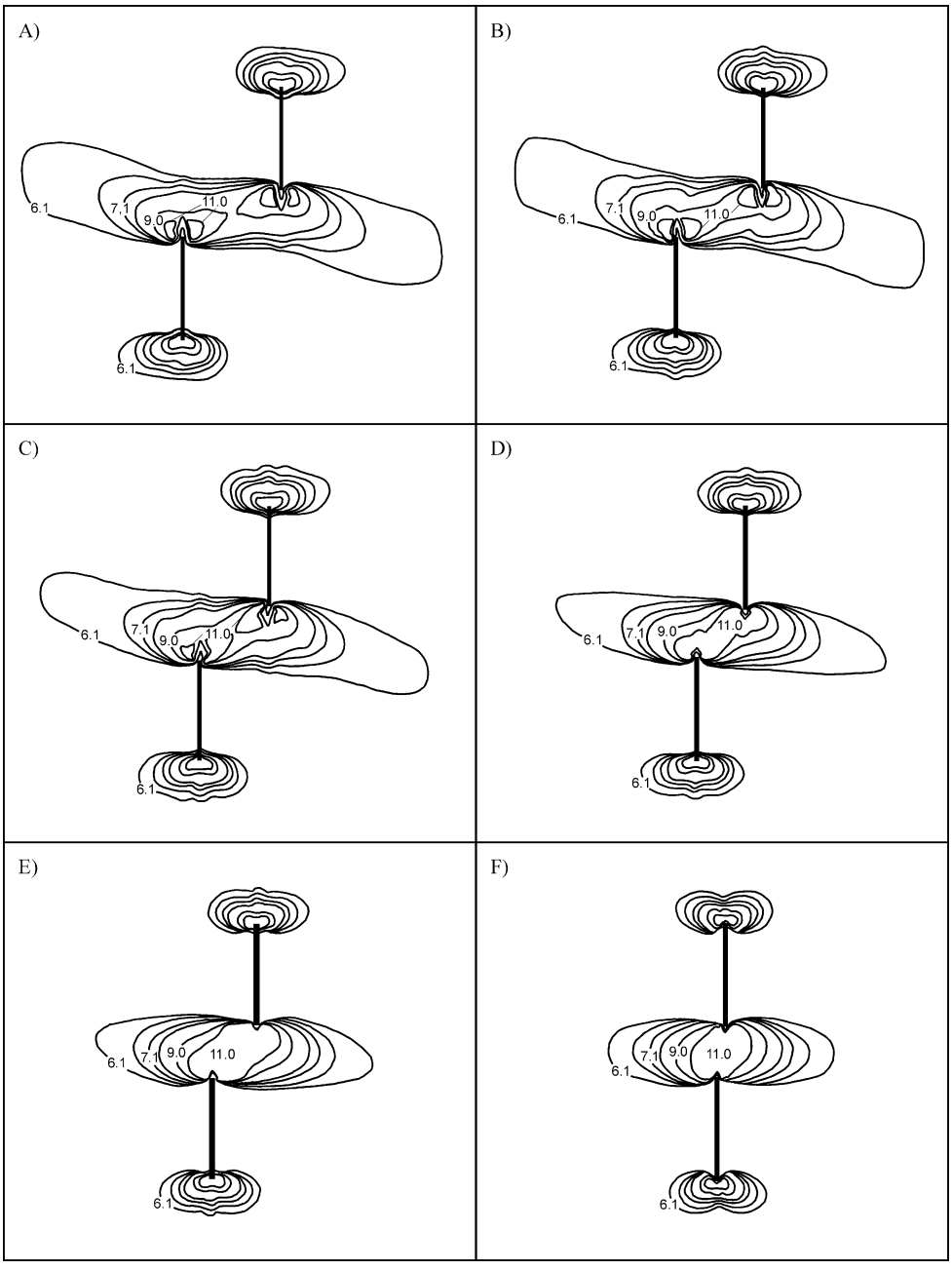

Fig. 19A–F Changes in tensile-stress concentration between the extension fractures in Fig. 16 when the offset b changes, whereas the underlap c is constant (same model as in Fig. 18). In **A**, b=1.0a and b gradually decreases (through models **B**–**E**) to 0.1a in **F**. The tensile stress generally increases as the offset decreases and the fractures become more nearly collinear. It follows that collinear fractures would tend to develop along extension or tension fractures

several ways. For example, the aquifer may be a highly overpressured artesian aquifer; alternatively, tectonic stresses such as horizontal extension parallel with the aquifer, or stresses related to active faulting, may reduce one of the horizontal principal stresses in the roof of the aquifer, so that it ruptures. This occurs when:

$$p_l + p_e = \sigma_3 + T_0 \tag{3}$$

where p_l is the lithostatic pressure (stress) at the depth of the aquifer; $p_e = P_t - p_l$ is the excess fluid pressure, that is, the difference between the total fluid pressure, P_t, in the aquifer at the time of the host-rock rupture and the lithostatic pressure; and σ_3 and T_0 are the minimum principal compressive stress and the in-situ tensile strength respectively in the host rock at the site of rupture.

If the host rock behaves elastically, then the aquifer (water sill) carries the entire weight of the rocks above and deforms as its fluid pressure changes. It can then be shown, using the special solution of the Navier-Stokes equation for flow between parallel plates (Lamb 1932; White 1979; Spence et al. 1987; Gudmundsson et al. 2002), that the volumetric flow rate along the vertical y-coordinate axis, Q_y, may be given by:

$$Q_y = \frac{b^3 W}{12\mu}\left[(\rho_r - \rho_f)\, g - \frac{\partial p_e}{\partial y}\right] \tag{4}$$

where b is the hydrofracture aperture, W is its width in a direction perpendicular to the flow direction (Fig. 20), ρ_r is the density of the host rock, ρ_f is the density and μ the

 DOI 10.1007/s10040-002-0238-0

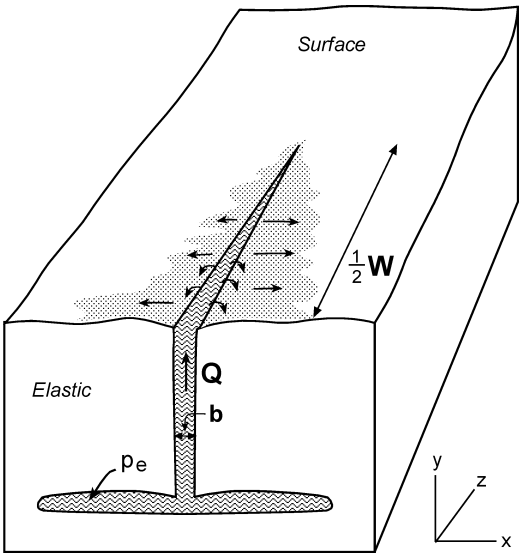

Fig. 20 Schematic illustration of a hydrofracture originating from a horizontal, elastic aquifer with an excess water pressure of p_e at the time of aquifer rupture. The volumetric flow rate Q, hydrofracture aperture b, and half width W are indicated

dynamic viscosity of the fluid, g is the acceleration due to gravity, p_e is the excess pressure defined in Eq. (3), and $\partial p_e/\partial y$ is the excess-pressure gradient in the flow direction. From these definitions it follows that the fracture cross-sectional area perpendicular to the flow is $A = bW$ The y-axis is positive upwards so that the first term on the right side of the equation is positive, even though the flow is in the direction of decreasing pressure, and the second term is negative. Because the host rock is considered elastic, the weight of the rock above the aquifer must be supported by its internal fluid pressure (Fig. 20). Consequently, the fluid flow is partly driven by buoyancy that springs from the density difference between the host rock and the fluid ($\rho_r - \rho_f$). In Eq. (4) the buoyancy term is added to the (negative) excess-pressure gradient $\partial p_e/\partial y$.

Equation (4), which applies to fluid transport in vertical hydrofractures, is easily modified so as to apply to faults with a certain dip angle α. Then the component of gravity in the dip direction of the fault is $g \sin \alpha$ so that Eq. (4) becomes:

$$Q_L = \frac{b^3 W}{12\mu}\left[(\rho_r - \rho_f)\, g \sin\alpha - \frac{\partial p_e}{\partial L}\right] \tag{5}$$

where ∂L is that part of the dip dimension of the fault along which the fluid flows at a volumetric rate Q_L, and the other symbols are as defined above. This equation can be generalised so as to take into account abrupt changes in fracture dip, as is common during the early stages of development of extension and shear fractures from en-echelon sets of joints.

Aperture Size in a Homogeneous Rock

Equations (4) and (5) show that volumetric fluid transport of a fracture depends on its aperture size, b, which in turn is a function of the fluid overpressure. The fluid overpressure itself, P_0, can vary along the plane of the hydrofracture. The overpressure variation depends on initial excess pressure, p_e, in the source aquifer (Eq. 3), the buoyancy term (Eqs. 4, 5), the local dip of the hydrofracture (Eq. 5), and the stress changes in the host rock. A general analytical solution for the aperture-size variation along a hydrofracture is obtained by considering a mathematical crack, a line crack, located along the vertical y-axis. In this solution, the effects of buoyancy, fracture dip, and host-rock stress are all included in the fluid-overpressure function. The crack is then defined by x=0, $-a \le y \le a$ and is supposed to be subject to an internal fluid overpressure given by the even function $p(y)=p(-y)$, so that the pressure is the same inside the fracture, above and below the x-axis.

The general solution for the normal displacement (half the aperture) of one crack wall in the direction of the x-axis, $u=u_x(y, 0)$, for various fluid-overpressure distributions, is given (Sneddon 1973; Maugis 2000) as:

$$u = \frac{4(1-\nu^2)}{\pi E}\int_y^a \frac{tq(t)dt}{(t^2-y^2)^{1/2}} \tag{6}$$

where ν is the Poisson's ratio and E the Young's modulus of the host rock, and

$$q(t) = \int_0^t \frac{p(y)dy}{(t^2-y^2)^{1/2}} \tag{7}$$

with $0<t<a$.

For constant fluid overpressure in the crack, we have $p(y) = P_0$, and Eq. (7) gives $q(t) = P_0\pi/2$. Substituting this for $q(t)$ in Eq. (6) and solving the integral, results in:

$$u = \frac{2(1-\nu^2)P_0}{E}(a^2-y^2)^{1/2} \tag{8}$$

This is the plane-strain formula for a two-dimensional, elliptic through crack, a "tunnel crack" (Sneddon and Lowengrub 1969; cf. Gudmundsson 2000b), showing that a constant fluid overpressure opens a hydrofracture in a homogeneous, isotropic rock into a flat ellipse.

When this model of a flat ellipse is used, the average aperture from measurements in the field is commonly similar to, and can be used for, the maximum aperture b_{max} of the hydrofracture. If one defines $b_{max} = 2u$ for the centre of the hydrofracture (where y=0) and the dimension $L = 2a$, then Eq. (8) simplifies to:

$$b_{max} = \frac{2P_0(1-\nu^2)L}{E} \tag{9}$$

which has often been applied in hydrofracture studies (Pollard and Segall 1987; Gudmundsson et al. 2002). For comparison, if the hydrofracture is modeled as a circular, interior (penny-shaped) crack, its maximum aperture is (Tada et al. 2000; cf. Gudmundsson 2000b):

$$b_{max} = \frac{8P_0(1-\nu^2)R}{\pi E} \tag{10}$$

where R is the radius of the crack and the other symbols are as defined above. Because the crack is here circular,

 DOI 10.1007/s10040-002-0238-0

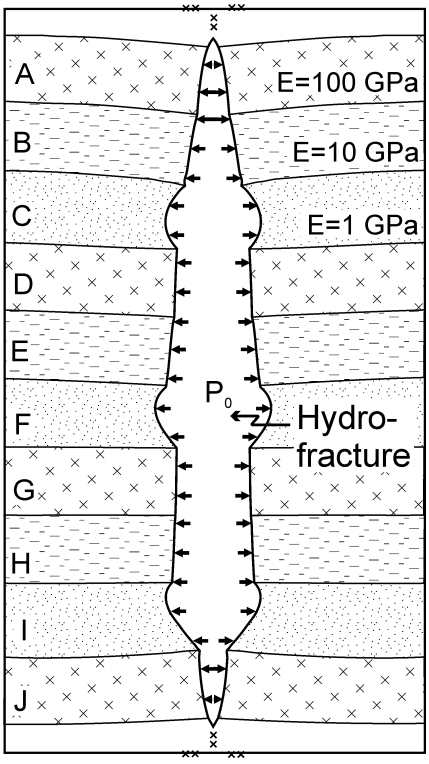

Fig. 21 Boundary-element model results for the aperture of a hydrofracture dissecting rock layers *A*–*J* with different Young's moduli. The hydrofracture is subject to a constant fluid overpressure of 6 MPa. The aperture size in the soft layers *C*, *F* and *I* is much greater than in the stiff (*A*, *D*, *G*, *J*) and moderately stiff (*B*, *E*, *H*) layers. Variation in aperture size normally encourages flow channeling

R can represent either half its dip dimension or half its strike dimension. Equations (9) and (10) show how the maximum aperture, b_{max}, of a hydrofracture depends on its controlling dimension (L or $2R$) as well as on the fluid overpressure P_0.

Aperture size in a Layered Rock

When the host rock is layered, many hydrofractures become arrested at the contacts between the layers (Figs. 4, 11; Gudmundsson and Brenner 2001) but some are still able to propagate through many layers. If the layers have different mechanical properties (Figs. 4, 6), the variation in aperture size of a hydrofracture can be very different from that presented for the homogeneous and isotropic rock above. In particular, the Young's moduli of the layers through which the hydrofracture propagates have large effects on the resulting aperture size. Layers with a low Young's modulus are referred to as soft and those with a high Young's modulus as stiff, as is traditional in engineering rock mechanics (Hudson and Harrison 1997).

A boundary-element model was made of the variation in aperture size in a fracture subject to constant fluid overpressure of 6 MPa but dissecting 10 layers with different Young's moduli. To bring these effects into focus, the Young's moduli used cover the normal static range for common rock types, that is, from 100 GPa for the stiff layers, through 10 GPa for the moderately stiff layers, to 1 GPa for the soft layers (Johnson 1970; Jumikis 1979; Afrouz 1992; Bell 2000).

The results (Fig. 21) show that the hydrofracture aperture is largest in the soft layers and smallest in the stiff layers. The great variation in aperture size indicates a strong tendency to flow channeling in unsaturated fracture pathways initially formed by hydrofracture propagation in rocks composed of layers with contrasting mechanical properties. As a consequence, groundwater transport in a direction perpendicular to the initial propagation direction of the hydrofracture would tend to be channeled to the part of the hydrofracture with the largest aperture.

Discussion

Groundwater transport in solid rocks is commonly largely, and sometimes entirely, controlled by the permeability of the associated fracture networks. For example, in a fractured but otherwise impermeable rock, all the groundwater transport would be along the fractures, irrespective of the hydraulic gradient. For groundwater flow to take place along a fracture network, the fractures must be interconnected in such a way that the percolation threshold is reached. In this paper, two mechanisms have been considered by which fracture networks, such as systems of joints, and contacts become interconnected.

One mechanism is the linking up of fractures in a rock subjected to tensile (or any other external) loading. If the original fractures are offset, they link up primarily through transverse-shear fractures but, if the original fractures are collinear, they link up through extension fractures. When such fracture sets reach certain crustal depths (Eq. 1), or otherwise become subject to shear stress, they may develop into shear fractures and, eventually, faults. The other mechanism is the growth of extension fractures as overpressured hydrofractures. The pathway of the hydrofracture is then primarily generated by opening up and linking contacts, joints, and other discontinuities in the host rock.

Both mechanisms assume the existence of outcrop-scale discontinuities, such as joints and contacts. This assumption is normally justified because most rocks contain joints, and many of these are generated during the formation of the rock. This applies in particular to igneous and sedimentary rocks. For example, columnar joints are very common in lava flows (Figs. 1, 2, and 13), from which larger fractures may develop by the mechanisms discussed above. Rock-mechanics experiments as well as field observations indicate that, in rocks under compressive stresses, shear fractures may form by a mechanism that does not involve the linking up of outcrop-scale discontinuities (Paterson 1978; Twiss and Moores 1992). A discussion of this mechanism, however, is beyond the scope of the present paper.

The numerical models presented here indicate how joint and fracture systems may link up into interconnect-

 DOI 10.1007/s10040-002-0238-0

ed fractures that can transport groundwater. Many of these systems subsequently develop into shear fractures and, eventually, large faults. The models presented here, however, deal only with the initiation of such shear fractures, and not with their subsequent development as faults. Repeated slip on faults normally leads to the development of two major hydromechanical units, namely, a fault-damage zone and a fault core (Caine et al. 1996; Evans et al. 1997; Seront et al. 1998). The fault-damage zone consists mainly of fractures of various sizes and is thus best treated as a fractured medium (Fig. 22). By contrast, the fault core is primarily composed of breccia and other cataclastic rocks and is best treated as a porous medium, except during fault slip when the core, or its contact with the damage zone, may fracture (Gudmundsson 2000a; Gudmundsson et al. 2002). The great influence that seismogenic faulting commonly has on groundwater flow (Roeloffs 1988; Muirwood and King 1993; Rojstaczer et al. 1995) is a topic that has received rather little attention in hydrogeology and needs to be explored in more detail.

In this paper, the numerical models of hydrofracture propagation focus on pathway formation where the entire fracture-forming fluid disappears subsequent to the fracture formation. This is presumably a common situation where the fracture-forming fluid is groundwater but, as a rule, it is not the case when the fluid is hydrothermal water or magma. Hydrothermal veins are very common in active fault zones (Gudmundsson et al. 2002). Although some veins may reach lengths of hundreds of metres (Bons 2001), presumably most have lengths of the order of metres or less (Gudmundsson et al. 2002). Thus, although mineral veins are commonly barriers to transverse groundwater flow, individually they are normally too small to have significant effects on regional groundwater flow.

Regional dykes are also emplaced as hydrofractures where the fluid is magma that becomes solidified in the fracture subsequent to its formation. Some dykes, particularly thick and massive ones, are barriers to transverse flow of groundwater. This follows because the dyke rock is commonly dense basalt of low matrix permeability. Other thick dykes, however, form in many magma injections, each of which may develop transverse columnar joints on solidification (Gudmundsson 1995). These dykes, some of which reach tens of metres in thickness, may be relatively permeable because of the columnar joints, and the same applies to many thin dykes. Thick, fractured dykes may act as sources of groundwater (Singhal and Gupta 1999). In some dykes, however, the columnar joints are partly, or entirely, filled with secondary minerals, in which case even thin dykes may be barriers to transverse groundwater flow.

Because the dyke rock has commonly very different mechanical properties from that of the host rock (granite, gneiss, sedimentary, and pyroclastic rocks), stresses tend to concentrate at the contacts between dykes and host rocks and generate groundwater conduits. Thus, dykes, even those that are barriers to transverse flow, are commonly good conduits of dyke-parallel flow of groundwater. Regional dykes that extend for many kilometres, or tens of kilometres, on strike and down the dip, can have very significant effects on the regional groundwater transport. In many areas, for example, in Iceland and Tenerife (Canary Islands), dykes collect groundwater and may transport it over long distances. Because the dykes are hydrofractures, they form groundwater pathways by linking up of discontinuities. Thus, groundwater flow along dykes follows pathways similar to those generated in the numerical models discussed above (Figs. 9, 10, 11, 12, and 14). It follows that the models presented here indicate not only the pathways of groundwater flow inside open hydrofractures, but also groundwater flow along the margin of dykes and other solidified hydrofractures.

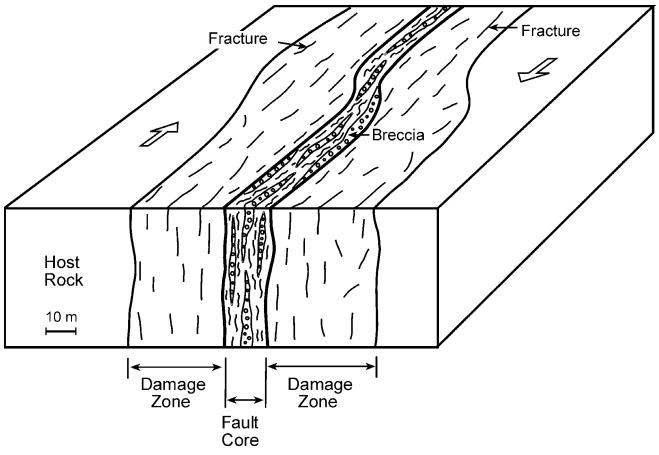

Fig. 22 Generalised infrastructure of a strike-slip fault consisting of two main units; a fault core and a fault-damage zone (cf. Gudmundsson et al. 2002). The core and its contact with the damage zone are the main displacement zones. The core consists primarily of breccia and other cataclastic rocks. The damage zone is located on each side of the core and contains numerous faults and fractures, many of which are eventually filled with secondary minerals, but it lacks large volumes of breccia. In major fault zones, the thickness of the core may be as much as several tens of metres and that of the damage zone many hundred metres or more

Acknowledgements We thank the Hydrogeology Journal referees for helpful comments. This work was supported by a grant from the European Commission (contract EVR1-CT-1999-40002), several grants from the Norway Research Council, and a PhD grant from Statoil (to Agust Gudmundsson) for Sonja L. Brenner.

References

Acocella V, Gudmundsson A, Funiciello R (2000) Interaction and linkage of extension fractures and normal faults: examples from the rift zone of Iceland. J Struct Geol 22:1233–1246

Afrouz AA (1992) Practical handbook of rock mass classification systems and modes of ground failure. CRC Press, London

Amadei B, Stephansson O (1997) Rock stress and its measurement. Chapman & Hall, London

Anderson EM (1951) Dynamics of faulting and dyke formation, 2nd edn. Olivier and Boyd, Edinburgh

 DOI 10.1007/s10040-002-0238-0

Atkins AG, Mai YW (1985) Elastic and plastic fracture. Horwood, Chichester, England
BEASY (1991) The boundary element analysis system user guide. Computational Mechanics, Boston, Massachussetts, USA
Bell FG (2000) Engineering properties of soils and rocks, 4th edn. Blackwell, Oxford
Bergerat F, Angelier J (2001) Mechanisms of the faults of 17 and 21 June earthquakes in the South Iceland Seismic Zone from the surface traces of the Arnes and Hestfjall faults. C R Acad Sci Paris 333:35–44
Bons PD (2001) The formation of large quartz veins by rapid ascent of fluids in mobile hydrofractures. Tectonophysics 226:1–17
Bruhn RL, Parry WT, Yonkee WA, Tompson T (1994) Fracturing and hydrothermal alteration in normal fault zones. Pure Appl Geophys 142:609–644
Caine JS, Evans JP, Forster CB (1996) Fault zone architecture and permeability structure. Geology 24:1025–1028
Cartwright JA, Trudgill BD, Mansfield CS (1995) Fault growth by segment linkage. An explanation for scatter in maximum displacement and trace length data from the Canyonlands Grabens of SE Utah. J Struct Geol 17:1319–1326
Chilingar GV, Robertson JO, Rieke HH (2002) Origin of abnormal formation pressures. In: Chilingar GV, Serebryakov VA, Robertson JO (eds) Origin and prediction of abnormal formation pressures. Elsevier, Amsterdam, pp 21–67
Cook J, Gordon JE (1964) A mechanism for the control of crack growth in all-brittle systems. Proc R Soc Lond A282:508–520
Cox SJD, Scholz CH (1988) On the formation and growth of faults: an experimental study. J Struct Geol 10:413–430
Crider JG, Pollard DD (1998) Fault linkage: three-dimensional mechanical interaction between echelon normal faults. J Geophys Res 103:24373–24391
Evans JP, Forster CB, Goddard JV (1997) Permeability of fault-related rocks and implications for hydraulic structure of fault zones. J Struct Geol 19:1393–1404
Faybishenko B, Witherspoon PA, Benson SM (eds) (2000) Dynamics of fluids in fractured rocks. American Geophysical Union, Washington, DC
Gentier S, Hopkins D, Riss J (2000) Role of fracture geometry in the evolution of flow paths under stress. In: Faybishenko B, Witherspoon PA, Benson SM (eds) Dynamics of fluids in f ractured rock. American Geophysical Union, Washington, DC, pp 169–184
Goodman RE (1989) Introduction to rock mechanics, 2nd edn. Wiley, New York
Gudmundsson A (1987a) Tectonics of the Thingvellir fissure swarm, SW Iceland. J Struct Geol 9:61–69
Gudmundsson A (1987b) Geometry, formation and development of tectonic fractures on the Reykjanes Peninsula, southwest Iceland. Tectonophysics 139:295–308
Gudmundsson A (1992) Formation and growth of normal faults at the divergent plate boundary in Iceland. Terra Nova 4:464–471
Gudmundsson A (1995) Geometry and growth of dykes. In: Baer G, Heimann A (eds) Physics and chemistry of dykes. Balkema, Rotterdam, The Netherlands, pp 23–34
Gudmundsson A (1999) Postglacial crustal doming, stresses and fracture formation with application to Norway. Tectonophysics 307:407–419
Gudmundsson A (2000a) Active fault zones and groundwater flow. Geophys Res Lett 27:2993–2996
Gudmundsson A (2000b) Fracture dimensions, displacements and fluid transport. J Struct Geol 22:1221–1231
Gudmundsson A, Brenner SL (2001) How hydrofractures become arrested. Terra Nova 13:456–462
Gudmundsson A, Brynjolfsson S, Jonsson MT (1993) Structural analysis of a transform fault-rift zone junction in North Iceland. Tectonophysics 220:205–221
Gudmundsson A, Fjeldskaar I, Brenner SL (2002) Propagation pathways and fluid transport of hydrofractures in jointed and layered rocks in geothermal fields. J Volcanol Geotherm Res 116:257–278
Haneberg WC, Mozley PS, Moore JC, Goodwin LB (eds) (1999) Faults and subsurface fluid flow in the shallow crust. American Geophysical Union, Washington, DC
Hubbert MK, Willis DG (1957) Mechanics of hydraulic fracturing. Am Inst Mining Eng Petrol Trans 210:153–188
Hudson JA, Harrison JP (1997) Engineering rock mechanics: an introduction to the principles. Pergamon, Oxford
Johnson AM (1970) Physical processes in geology. Freeman, Cooper & Company, San Francisco, California, USA
Jumikis AR (1979) Rock mechanics. Trans Tech Publications, Clausthal, Germany
Lamb H (1932) Hydrodynamics, 6th edn. Cambridge University Press, Cambridge
Mansfield C, Cartwright J (2001) Fault growth by linkage: observations and implications from analogue models. J Struct Geol 23:745–763
Maugis D (2000) Contact, adhesion and rupture of elastic solids. Springer, Berlin Heidelberg New York
Muirwood R, King GCP (1993) Hydrologic signatures of earthquake strain. J Geophys Res 98:22035–22068
Paterson MS (1978) Experimental rock deformation. The Brittle Field. Springer, Berlin Heidelberg New York
Peacock DCP, Sanderson DJ (1999) Deformation history and basin-controlling faults in the Mesozoic sedimentary rocks of the Somerset coast. Proc Geol Assoc 110:41–52
Pollard DD, Segall P (1987) Theoretical displacements and stresses near fractures in rock: with application to faults, joints, veins, dikes and solution surfaces. In: Atkinson B (ed) Fracture mechanics of rock. Academic Press, London, pp 277–349
Priest SD (1993) Discontinuity analysis for rock engineering. Chapman & Hall, London
Roeloffs EA (1988) Hydraulic precursors to earthquakes: a review. Pure Appl Geophys 126:177–209
Rojstaczer S, Wolf S, Michel R (1995) Permeability enhancement in the shallow crust as a cause of earthquake-induced hydrological changes. Nature 373:237–239
Secor DT (1965) The role of fluid pressure in jointing. Am J Sci 263:633–646
Selley RC (1998) Elements of petroleum geology. Academic Press, New York
Seront B, Wong TF, Caine JS, Forster CB, Bruhn RL (1998) Laboratory characterisation of hydromechanical properties of a seismogenic normal fault system. J Struct Geol 20:865–881
Singhal BBS, Gupta RP (1999) Applied hydrogeology of fractured rocks. Kluwer, London
Sneddon IN (1973) Integral transform methods. In: Sih GC (ed) Mechanics of fracture. I. Methods of analysis and solutions of crack problems. Nordhoff, Leyden, pp 315–367
Sneddon IN, Lowengrub M (1969) Crack problems in the classical theory of elasticity. Wiley, New York
Spence DA, Sharp PW, Turcotte DL (1987) Buoyancy-driven crack propagation: a mechanism for magma migration. J Fluid Mech 174:135–153
Tada H, Paris PC, Irwin GR (2000) The Stress analysis of cracks handbook, 3rd edn. Del Research Corporation, Hellertown, Pennsylvania, USA
Timoshenko SP, Goodier JN (1970) Theory of elasticity, 3rd edn. McGraw-Hill, London
Twiss RJ, Moores EM (1992) Structural geology. WH Freeman, New York
van der Pluijm BA, Marshak S (1997) Earth structure. McGraw-Hill, New York
White FM (1979) Fluid mechanics. McGraw-Hill, New York

 DOI 10.1007/s10040-002-0238-0